


High-resolution separation of bioisomers using ion cloud profiling

Received: 17 September 2022

Xiaoyu Zhou ^{1,2}, Zhuofan Wang¹, Jingjin Fan¹ & Zheng Ouyang ^{1,2} ✉

Accepted: 9 March 2023

Published online: 20 March 2023

 Check for updates

Elucidation of complex structures of biomolecules plays a key role in the field of chemistry and life sciences. In the past decade, ion mobility, by coupling with mass spectrometry, has become a unique tool for distinguishing isomers and isoforms of biomolecules. In this study, we develop a concept for performing ion mobility analysis using an ion trap, which enables isomer separation under ultra-high fields to achieve super high resolutions over 10,000. The potential of this technology has been demonstrated for analysis of isomers for biomolecules including disaccharides, phospholipids, and peptides with post-translational modifications.

Biomolecules, such as glycans, lipids, and peptides, play vital roles in biological systems^{1–3}. They exist in forms of a wide variety of isomers or isoforms, which have identical chemical formulas and molecular weights but different structures and biological functions⁴. The glycans^{5–9} and lipids^{10–12} have complex configurations, while the structural characterization of peptides and proteins can be complicated with post-translational modifications (PTMs) and higher-order conformations, all resulting in a variety of isomers and isoforms^{13–15}. The significance of identifying isomers is well recognized for almost all disciplines¹⁶. As one example, isomers such as cis or trans unsaturated fatty acids in food can have very different effects on human health¹⁷.

Ionic forms of the molecules have been used as surrogates for species identification as well as structural characterization. While mass spectrometry (MS) is often used to obtain the compositions of molecular ions^{18–21}, ion mobility (IM) has been widely employed for differentiation of the isomers and isoforms of biomolecular ions^{22–24}. The combination of these two technologies in the form of IM-MS has been a major direction in mass spectrometry development during the last decade. IM techniques separate ions based on the mobility differences due to the collisions between the ions and the background neutral molecules. Taking the most classic method with drift-tube ion mobility as an example, it uses ion-neutral collisions in an electric field (with a field strength E) to identify the differences in collision cross-section (CCS), which is associated with the variations in structures of molecular ions. Applications of IM have led to the separation of the isomers or isoforms for disaccharides, phospholipids, and peptides with post-translational modifications^{25–27}. The separation efficiency is affected by

both the electric field E and the number density (N) of the collision gas. The mobility of the ions is the result of the balance between the motion driven by the electric field E and the collisions with the background gas molecules. Typically, IM is performed under a low electric field $E/N < 30$ Td (Townsend number, $1\text{ Td} = 1 \times 10^{-21} \text{ V m}^2$)²⁸, such as for implementations with drift time²², traveling wave²⁹, trapped^{30, 31}, and differential modes³². With a long separation time³⁰ or path^{33–36}, separation resolutions of several hundreds have been achieved (Supplementary Fig. 1 and Supplementary Table 1), which, however, is still inadequate for differentiating bioisomers of high structural complexities.

Operating the IM at higher E/N ratios, for example, applying high-field asymmetric waveform at -100 Td, shows enhanced isomer separation;³⁷ however, researchers have not discovered an effective method for implementation with higher E/N ratios. The main challenge is to prevent the loss of the ions while they are driven by a high electric field through the collisions over a relatively long time or long path.

Here, we report the development of ion cloud profiling technology to enable high-resolution IM analysis in a radiofrequency (RF) electromagnetic field with $E/N > 1$ MTd. Isomer differentiation was achieved at a resolution better than 10,000, which allowed us to attack some challenging issues in the structural analysis of biomolecules.

Results and discussion

Ion cloud profiling: instrumentation and performance

The ion cloud profiling was performed in a dual-LIT (linear ion trap) miniature mass spectrometer modified from a Mini β instrument

¹State Key Laboratory of Precision Measurement Technology and Instruments, Department of Precision Instrument, Tsinghua University, Beijing 100084, China. ²Institute for Precision Medicine, Tsinghua University, Beijing 100084, China. ✉e-mail: ouyang@tsinghua.edu.cn

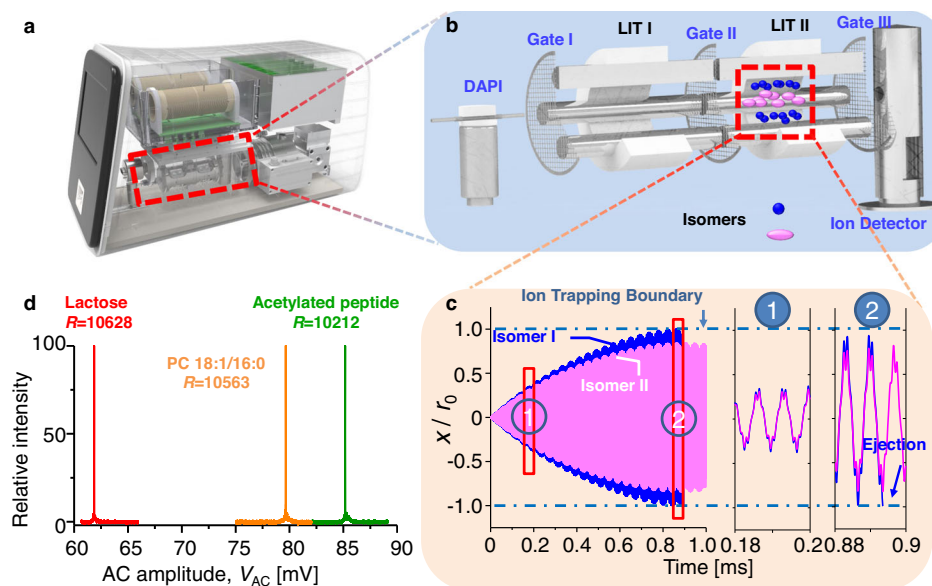


Fig. 1 | Instrumental setup, principal, and performance characterization of the ion cloud profiling technology. Schematics of **a** the miniature MS system used in this work and **b** its key components for isomer structural analysis. **c** Simulated ion trajectories for two isomeric ions characterized by reduced damping coefficients: $b' = 0.0010$ (blue) and 0.0012 (purple). Here, $b' = 2b/\Omega m$, where Ω is the angular frequency of the RF field, m is ion mass, b is the damping coefficient of the ions. Insets, zoom-in plots of the ion trajectories at the beginning (1) and ejection (2) stages of the AC excitation. Isomeric ions are ejected sequentially according to their DCSs when their oscillation amplitudes exceed the trap geometry, r_0 , as

indicated by the blue dashed lines. **d** Ion cloud profiling spectra of three biomolecules, lactose (m/z 365, CCS 177.6 \AA^2), phosphatidylcholine (PC) 18:1/16:0 (m/z 761, CCS 296.2 \AA^2), and an acetylated peptide (m/z 542, CCS 357.9 \AA^2), superimposed in one spectrum. The CCS values of lactose and peptide are measured by timsTOF (Bruker Daltonics, Bremen, Germany). The CCS value of phosphatidylcholine is taken from *Groessl's* work⁴². The resolution here is defined as, $R = V_{AC}/\Delta V_{AC}$, where V_{AC} and ΔV_{AC} are the AC ejection amplitude of analyte ions and the full width at half maximum (FWHM) of the peak, respectively⁴³.

(PURSPEC Technology (Beijing) Ltd., Beijing China) (Fig. 1a), which is also capable of performing tandem MS analysis³⁸. Ions of isomers were generated by a nano-electrospray ionization (nESI) source, mass selected in the LIT I, and transferred to the LIT II for final structural analysis (Fig. 1b). The physics employed here was that under forced oscillations, ion clouds of the isomeric ions were separated due to their difference of damping cross-sections (DCSs, Fig. 1c)^{39–41}. For experimental implementations, an auxiliary alternative-current (AC) was employed for resonance excitation of the isomeric ions in the LIT; by scanning the AC voltages in different scan rates depending on the species, the isomeric ions with different DCSs were ejected sequentially according to the ion cloud profile sizes (Fig. 1c and Supplementary Fig. 2). When the AC scanning speed was below 5000 mV/s , a good correlation between AC ejection voltages and DCSs could be established and an ion cloud profiling spectrum with a resolution over 10000 (Fig. 1d) was produced. More specifically, the AC scanning speed was 53 mV/s for the analysis of disaccharides, and 88 mV/s for both phospholipids and peptides (Fig. 1d).

Analysis of biomolecules

To show the enhanced separation capability of the technology, we first analyzed glycans with complexed isomeric structures. Four disaccharides, including trehalose, maltose, cellose, and lactose, were considered. They present differences in the structure include composition, connectivity, and configuration (Fig. 2a). The disaccharides are composed of basic building blocks, the monosaccharides. Each monosaccharide contains multiple hydroxyl groups, which could be connected to form a glycosidic bond with another monosaccharide. Through linking different hydroxyl groups, carbohydrates normally have branched structures with diverse regiochemistry. In addition, each glycosidic bond formation is accompanied by creation of a stereocenter, because two monosaccharides could be connected via two different configurations. Using ion cloud profiling method developed here, the four isomeric disaccharides were baseline resolved (Fig. 2b)

and the experimental results agreed well with the simulation (Supplementary Fig. 3). A mixture of lactose and cellose was also analyzed, by both IM through ion cloud profiling (Fig. 2c) and MS/MS analysis (Top, Fig. 2d). While MS/MS normally is powerful for distinguish isomers through characteristic fragmentation patterns, in this case identical patterns were observed for these two isomers. The results here suggest that the IM using ion cloud profiling technology is complementary to the MS or MS/MS analysis and has the potential to achieve high-resolution structural analysis of isomers, leading to isomeric-specific selection (Supplementary Fig. 4) and quantification analysis (Figs. 2e and 2f).

To show the universality of the technology, we further demonstrated the structural separation of phospholipids (Fig. 3a) and peptides (Fig. 3e). Phospholipids consist of two fatty acyl chains, a phosphate head group, and a glycerol backbone, for which the isomerization arises from a number of variants in structure including sn-positions of the fatty acyl chains (Fig. 3b), C=C locations (Fig. 3c) and configurations (cis/trans, Fig. 3d) of C=C in each fatty acyl chain, derivatization sites, and etc. These structure features could be well characterized using the ion cloud profiling (Fig. 3b–d). For proteins and peptides, PTMs contribute significantly to the structure complexity. In this study, peptides SGKLRASHKG with methylation in K3 or K9 (Fig. 3f), acetylation in K3 or K9 (Fig. 3g), and phosphorylation in S1 or S7 (Fig. 3h) were analyzed for demonstration. As shown in Fig. 3f–h, the isomers of the peptides could all be clearly resolved in the ion cloud profiling spectra. This method has also been applied for distinguishing different conformations of protein ions, for which baseline separation was obtained for charge states of +9 and +13 of myoglobin as well as +12 and +13 for cytochrome c (Supplementary Fig. 5).

In summary, we show an ion mobility technology for high-resolution structural separation of bioisomers. The DCS-based ion cloud profiling could serve as an alternative means for structural separation of biomolecules. The technology developed here showed distinct advantages with a resolution over 10,000, which represents a

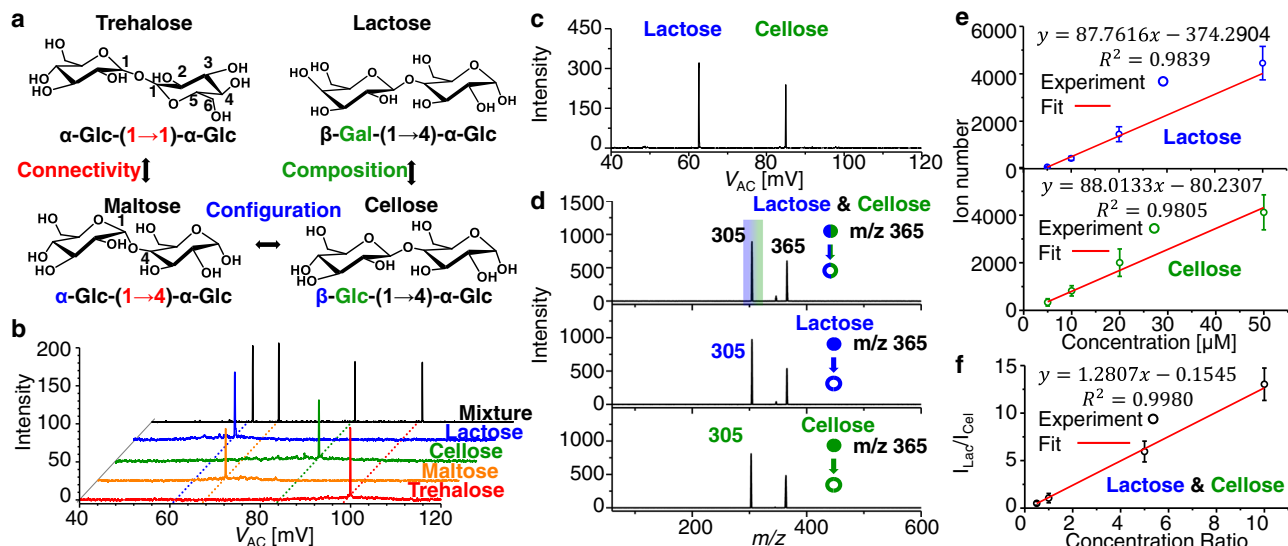


Fig. 2 | Structural analysis of glycans. **a** Structures of four isomeric disaccharides, which have isomerization of composition, connectivity, and configuration in pairs. **b** Ion cloud profiling spectra of the four disaccharides: trehalose (red), maltose (orange), cellose (green), lactose (blue), and the mixture of these four (black). **c** Ion cloud profiling spectrum of lactose and cellose mixture. **d** Tandem MS spectra of lactose and cellose mixture (top), pure lactose (middle), and pure cellose (bottom). Lactose (blue) and cellose (green) have identical mass to charge ratio, m/z

365, and fragment, m/z 305, in tandem MS spectra. **e** Calibration curves for pure lactose and cellose. For quantitative analysis of pure sample, concentrations varied from 5 μM to 50 μM . Each value represents the mean \pm s.d. ($N=10$). **f** Calibration curves for the mixture of lactose and cellose. For quantitative analysis of mixture, concentration of cellose was 5 μM , and concentration ratios of lactose to cellose varied from 0.5 to 10. Each value represents the mean \pm s.d. ($N=15$). Source data are provided as a Source Data file.

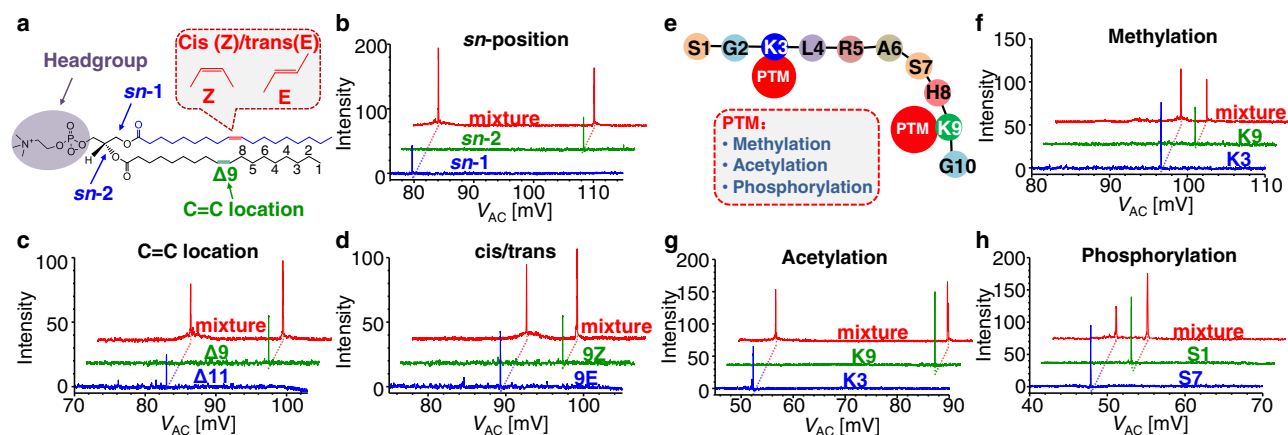


Fig. 3 | Structural analysis of lipids and peptides. **a** Structure of phospholipids with isomerization of *sn* position, carbon-carbon double bond location, and *cis/trans* structure due to the double bond. Ion cloud profiling spectra of **b** PC 18:1(9Z)/16:0 (blue), PC 16:0/18:1(9Z) (green), and their mixture (red); **c** PC 18:1(11Z)/18:1(11Z) (blue), PC 18:1(9Z)/18:1(9Z) (green), and their mixture (red); **d** PC 18:1(9E)/

18:1(9E) (blue), PC 18:1(9Z)/18:1(9Z) (green), and their mixture (red). **e** Structure of peptide, SGKLRASHKG, with different types of PTMs. Ion cloud profiling spectra of the peptide with **f** methylation in K3 (blue), K9 (green), and their mixture (red); **g** acetylation in K3 (blue), K9 (green), and their mixture (red); **h** phosphorylation in S1 (blue), S7 (green), and their mixture (red).

significant improvement in analytical technology for biological studies (Supplementary Fig. 1). Moreover, the implementation is very simple with the use of an ion trap, which can perform MS/MS analysis at the same time. Ion trap also is a popular ion processing device in modern hybrid mass spectrometers and the high E/N IM separation performed at low pressure make it highly compatible with coupling to mass analyzers such as Orbitrap and TOF. It is expected that this method can be readily applied for a broad range of applications for biological study.

Methods

Materials

Trehalose (200 μM) was purchased from Klamar reagent (Shanghai, China), maltose (200 μM) was purchased from Meryer (Shanghai, China), cellose (200 μM) was purchased from Macklin (Shanghai,

China), lactose (200 μM) was purchased from Aladdin (Shanghai, China). Synthetic lipids standards, PC 16:0/18:1(9Z) (200 μM), PC 18:0/16:1(9Z) (200 μM), PC 18:1/18:1(9Z) (200 μM), PC 18:1/18:1(9E) (200 μM) and PC 18:1/18:1(11Z) (200 μM), were purchased from Avanti Polar Lipids (Alabaster, AL, USA). Six kinds of peptides (50 μM), SGKLRASHKG with phosphorylation in S1 and S7, methylation in K3 and K9, acetylation in K3 and K9, were synthesized and purchased from Sangon Biotech (Shanghai, China). These samples were used directly without further purification. Methanol and water, purchased from Fisher Scientific (Fairlawn, NJ, USA) were used for preparing the sample solvents. Trehalose, maltose, cellose, lactose and six peptides were solvated in methanol and water (50/50, v/v). Lipids standards were solvated in methanol with 0.1% acetic acid.

MS instrumentation

The experiments were performed in a home-made dual-linear ion trap (dual-LIT) miniature MS system (Fig. 1a)³⁸, which includes a nano-electrospray (nESI) ion source for sample ionization in atmosphere, a discontinuous atmospheric pressure interface (DAPI) connecting the atmosphere and the vacuum, and dual-LIT mass analyzers, LIT I and LIT II, as well as three gates for ion processing. The DAPI uses a pinch valve to control the ion introduction during each analysis. The DAPI typically opens 5–30 ms to allow the ion introduction and then closes to allow the pressure drop back from 0.1 Torr (13.3 Pa) to 1×10^{-5} Torr. Each of the LITs had a nominal radius r_0 of 4 mm, and a length z_0 of 51 mm, driven by a dual-phase RF at a frequency of 1 MHz for ion trapping and mass analysis. The two LITs were separated by three mesh gates, which were applied with direct-current (DC) voltages to tune the ion transfer along the z direction (Table S2). With a small alternating-current (AC) voltages coupled with the RF, resonance excitation of the ions in the LITs was achieved to allow ion isolation, ion activation, and ion ejection (Table S3). Air was used as the buffer for ion cooling. For IM technique, typically the detector response speed is not the limiting factor for the resolution and the instrument operation status is not approaching the detector response speed limit. All data were collected and processed by SpecMS from PURSPEC. All data processing were performed using MATLAB 2017b from MathWorks.

Theoretical modeling and numeric simulations

Theoretical modeling and numeric simulations were employed for the understanding and optimization of the profiling process. When the ions were excited by an AC, the motion of the ions in the LIT II was described by a forced oscillation. The equation yields:

$$m \frac{d^2x}{dt^2} + b \frac{dx}{dt} + kx = C \sin(\omega t) \quad (1)$$

where m is ion mass, x is ion displacement in the x -coordinate, t is time. C represents the excitation strength and is defined as

$$C = \alpha V_{AC} / 2r_0 \quad (2)$$

where V_{AC} is AC voltage with an angular frequency ω and α is calibration coefficient. k is the spring constant due to the effective RF field and is defined as

$$k = 2eV_{eff} / r_0^2 \quad (3)$$

where V_{eff} is the effective trapping depth of the RF field, e is electron charge, and r_0 is the field radius of the LIT II. b is the damping coefficient of the ion motion and is defined as

$$b = eK^{-1} \quad (4)$$

K is the ion mobility in the RF field and is defined as

$$K = \frac{3e}{16N} \sqrt{\frac{2\pi}{\mu k_B T}} \frac{1}{\Omega_D} \quad (5)$$

where Ω_D is the DCS of the ions, k_B is Boltzmann constant, and μ is the reduced mass of ions and collision gas, T is temperature.

Therefore, the damping coefficient b is proportional to the damping cross-section from Eq. 4, and Eq. 5:

$$b = \frac{16N}{3} \sqrt{\frac{\mu k_B T}{2\pi}} \Omega_D \quad (6)$$

The solution of Eq. 1 yields:

$$x = \gamma e^{-\frac{b}{2m}t} \sin\left(\sqrt{\omega_0^2 - \frac{b^2}{4m^2}}t + \delta\right) + \left[\frac{(\omega_0^2 - \omega^2)\sin(\omega t) - \frac{b\omega}{m}\cos(\omega t)}{(\omega_0^2 - \omega^2)^2 + \left(\frac{b\omega}{m}\right)^2}\right] \frac{C}{m} \quad (7)$$

where $\omega_0^2 = \frac{k}{m}$, γ and δ are arbitrary constant depending on the initial conditions of the ions. The first term represents a damped ion motion, whose oscillation amplitude goes to zero within a few milliseconds. The second term represent the forced oscillation of the ions. At resonance, i.e., $\omega = \omega_0$ (resonance frequency), the maximum displacement of the ion motion, A , as a function of the damping term, b , yields:

$$A = \frac{C}{b\omega_0} = \sigma b^{-1} \propto \Omega_D^{-1} \quad (8)$$

where $\sigma = C\sqrt{\frac{m}{k}}$ is a constant for a specific ion trapping condition.

Equation 8 is the theoretical basis of the ion cloud profiling technology for performing structural analysis of isomeric ions. Under the same AC excitation, the size of the ion cloud, A , becomes different for isomers according to the damping term b or DCS Ω_D , as shown in Fig. 1c.

Especially, if the displacement of the ion motion is equal to r_0 , we can obtain the correlation between scanning AC voltage and DCS Ω_D , which has

$$V_{AC} = \frac{32N}{3} \sqrt{\frac{\mu k_B T}{2\pi}} \alpha^{-1} r_0^2 \omega_0 \Omega_D \quad (9)$$

The DCS of ions is proportional to the AC ejection voltage. And the larger the DCS is, the greater the AC ejection voltage is required.

To obtain the high E/N condition, the pressure for the analysis was set below 1×10^{-5} Torr. Adequate separation of isomers could be achieved, while the ion pack being maintained compact for each species (Supplementary Fig. 2) to allow high resolutions to be achieved through the ion cloud profiling method. For experimental implementation, high-resolution spectra were obtained by profiling the isomeric ion clouds at conditions optimized (Fig. 1d, Supplementary Figs. 6–10).

Reporting summary

Further information on research design is available in the Nature Portfolio Reporting Summary linked to this article.

Data availability

All data supporting the findings of this study are available from the corresponding authors upon request. The raw data are available from Figshare (<https://doi.org/10.6084/m9.figshare.22139816.v1>). Source data are provided with this paper.

Code availability

The codes used for data acquisition and processing are available from the corresponding authors upon request. The codes used for simulation are available from Github (<https://github.com/isShuaiLi/QIT.git>).

References

1. Dwek, R. A. Glycobiology: toward understanding the function of sugars. *Chem. Rev.* **96**, 683–720 (1996).
2. Saliba, A. E., Vonkova, I. & Gavin, A. C. The systematic analysis of protein-lipid interactions comes of age. *Nat. Rev. Mol. Cell Biol.* **16**, 753–761 (2015).
3. Mann, M. & Jensen, O. N. Proteomic analysis of post-translational modifications. *Nat. Biotechnol.* **21**, 255–261 (2003).

- Shevchenko, A. & Simons, K. Lipidomics: coming to grips with lipid diversity. *Nat. Rev. Mol. Cell Biol.* **11**, 593–598 (2010).
- Bentley, K. W., Nam, Y. G., Murphy, J. M. & Wolf, C. Chirality sensing of amines, diamines, amino acids, amino alcohols, and alpha-hydroxy acids with a single probe. *J. Am. Chem. Soc.* **135**, 18052–18055 (2013).
- Hart, G. W. & Copeland, R. J. Glycomics hits the big time. *Cell* **143**, 672–676 (2010).
- Gray, C. J. et al. Advancing solutions to the carbohydrate sequencing challenge. *J. Am. Chem. Soc.* **141**, 14463–14479 (2019).
- Hofmann, J., Hahm, H. S., Seeberger, P. H. & Pagel, K. Identification of carbohydrate anomers using ion mobility–mass spectrometry. *Nature* **526**, 241–244 (2015).
- Hofmann, J. & Pagel, K. Glycan analysis by ion mobility-mass spectrometry. *Angew. Chem.-Int. Edit.* **56**, 8342–8349 (2017).
- Cao, W. et al. Large-scale lipid analysis with C=C location and sn-position isomer resolving power. *Nat. Commun.* **11**, 375 (2020).
- Ma, X. X. & Xia, Y. Pinpointing double bonds in lipids by paterno-buchi reactions and mass spectrometry. *Angew. Chem.-Int. Edit.* **53**, 2592–2596 (2014).
- Williams, P. E., Klein, D. R., Greer, S. M. & Brodbelt, J. S. Pinpointing double bond and sn-positions in glycerophospholipids via hybrid 193 nm ultraviolet photodissociation (UVPD) mass spectrometry. *J. Am. Chem. Soc.* **139**, 15681–15690 (2017).
- Ruotolo, B. T. et al. Evidence for macromolecular protein rings in the absence of bulk water. *Science* **310**, 1658–1661 (2005).
- Laganowsky, A. et al. Membrane proteins bind lipids selectively to modulate their structure and function. *Nature* **510**, 172–175 (2014).
- Smith, D. P., Radford, S. E. & Ashcroft, A. E. Elongated oligomers in beta(2)-microglobulin amyloid assembly revealed by ion mobility spectrometry-mass spectrometry. *Proc. Natl. Acad. Sci. USA* **107**, 6794–6798 (2010).
- Ortiz, A. & Sanchez-Nino, M. D. The human plasma lipidome. *N. Engl. J. Med.* **366**, 668–669 (2012).
- de Souza, R. J. et al. Intake of saturated and trans unsaturated fatty acids and risk of all cause mortality, cardiovascular disease, and type 2 diabetes: systematic review and meta-analysis of observational studies. *BMJ* **351**, h3978 (2015).
- Cooks, R. G., Ouyang, Z., Takats, Z. & Wiseman, J. M. Ambient mass spectrometry. *Science* **311**, 1566–1570 (2006).
- Glish, G. L. & Vachet, R. W. The basics of mass spectrometry in the twenty-first century. *Nat. Rev. Drug Discov.* **2**, 140–150 (2003).
- McLuckey, S. A. & Wells, J. M. Mass analysis at the advent of the 21st century. *Chem. Rev.* **101**, 571–606 (2001).
- Tamara, S., den Boer, M. A. & Heck, A. J. R. High-resolution native mass spectrometry. *Chem. Rev.* **122**, 7269–7326 (2022).
- Lanucara, F., Holman, S. W., Gray, C. J. & Eyers, C. E. The power of ion mobility-mass spectrometry for structural characterization and the study of conformational dynamics. *Nat. Chem.* **6**, 281–294 (2014).
- Kanu, A. B., Dwivedi, P., Tam, M., Matz, L. & Hill, H. H. Ion mobility-mass spectrometry. *J. Mass Spectrom.* **43**, 1–22 (2008).
- Kalenius, E., Groessl, M. & Rissanen, K. Ion mobility-mass spectrometry of supramolecular complexes and assemblies. *Nat. Rev. Chem.* **3**, 4–14 (2019).
- Dodds, J. N. & Baker, E. S. Ion mobility spectrometry: fundamental concepts, instrumentation, applications, and the road ahead. *J. Am. Soc. Mass Spectrom.* **30**, 2185–2195 (2019).
- Gabelica, V. et al. Recommendations for reporting ion mobility mass spectrometry measurements. *Mass Spectrometry Rev.* **38**, 291–320 (2019).
- Kirk, A. T., Bohnhorst, A., Raddatz, C.-R., Allers, M. & Zimmermann, S. Ultra-high-resolution ion mobility spectrometry—current instrumentation, limitations, and future developments. *Anal. Bioanal. Chem.* **411**, 6229–6246 (2019).
- Cumeras, R., Figueras, E., Davis, C. E., Baumbach, J. I. & Gracia, I. Review on ion mobility spectrometry. Part 1: current instrumentation. *Analyst* **140**, 1376–1390 (2015).
- Chen, T. C. et al. Mobility-selected ion trapping and enrichment using structures for lossless ion manipulations. *Anal. Chem.* **88**, 1728–1733 (2016).
- Fouque, K. J. D. et al. Effective liquid chromatography-trapped ion mobility spectrometry-mass spectrometry separation of isomeric lipid species. *Anal. Chem.* **91**, 5021–5027 (2019).
- Dziekonski, E. T., Johnson, J. T., Lee, K. W. & McLuckey, S. A. Determination of collision cross sections using a Fourier transform electrostatic linear ion trap mass spectrometer. *J. Am. Soc. Mass Spectrom.* **29**, 242–250 (2018).
- Andrzejewski, R., Entwistle, A., Giles, R. & Shvartsburg, A. A. Ion mobility spectrometry of superheated macromolecules at electric fields up to 500 Td. *Anal. Chem.* **93**, 12049–12058 (2021).
- Deng, L. L. et al. Serpentine ultralong path with extended routing (SUPER) high resolution traveling wave ion mobility-MS using structures for lossless ion manipulations. *Anal. Chem.* **89**, 4628–4634 (2017).
- Hollerbach, A. L. et al. Ultra-high-resolution ion mobility separations over extended path lengths and mobility ranges achieved using a multilevel structures for lossless ion manipulations module. *Anal. Chem.* **92**, 7972–7979 (2020).
- Giles, K. et al. A cyclic ion mobility-mass spectrometry system. *Anal. Chem.* **91**, 8564–8573 (2019).
- Merenbloom, S. I., Glaskin, R. S., Henson, Z. B. & Clemmer, D. E. High-resolution ion cyclotron mobility spectrometry. *Anal. Chem.* **81**, 1482–1487 (2009).
- Guevremont, R. High-field asymmetric waveform ion mobility spectrometry: a new tool for mass spectrometry. *J. Chromatogr. A* **1058**, 3–19 (2004).
- Liu, X. W., Wang, X., Bu, P. X., Zhou, X. Y. & Zheng, O. Y. Tandem analysis by a dual-trap miniature mass spectrometer. *Anal. Chem.* **91**, 1391–1398 (2019).
- Cleven, C. D., Cooks, R. G., Garrett, A. W., Nogar, N. S. & Hemberger, P. H. Radial distributions and ejection times of molecular ions in an ion trap mass spectrometer: a laser tomography study of effects of ion density and molecular type. *J. Phys. Chem.* **100**, 40–46 (1996).
- Plass, W. R., Gill, L. A., Bui, H. A. & Cooks, R. G. Ion mobility measurement by dc tomography in an rf quadrupole ion trap. *J. Phys. Chem. A* **104**, 5059–5065 (2000).
- Snyder, D. T., Peng, W. P. & Cooks, R. G. Resonance methods in quadrupole ion traps. *Chem. Phys. Lett.* **668**, 69–89 (2017).
- Groessl, M., Graf, S. & Knochenmuss, R. High resolution ion mobility-mass spectrometry for separation and identification of isomeric lipids. *Analyst* **14**, 6904–6911 (2015).
- Ruotolo, B. T., Benesch, J. L. P., Sandercock, A. M., Hyung, S. J. & Robinson, C. V. Ion mobility-mass spectrometry analysis of large protein complexes. *Nat. Protoc.* **3**, 1139–1152 (2008).

Acknowledgements

We thank professor Yu Xia, Xiaoxiao Ma, and Wenpeng Zhang at Tsinghua University for their helpful discussions. This work was supported by the National Natural Science Foundation (Project No. 21627807 (Z.O.) and 21934003 (Z.O.)) and Tsinghua University Initiative Scientific Research Program of Precision Medicine. We also thank PURSPEC Technology (Beijing) Ltd. for support to instrument modification.

Author contributions

X.Z. and Z.O. designed the research; X.Z., Z.W., and J.F. performed the investigation; X.Z. and Z.O. wrote and edited the manuscript.

Competing interests

The authors declare no competing interests.

Additional information

Supplementary information The online version contains supplementary material available at <https://doi.org/10.1038/s41467-023-37281-7>.

Correspondence and requests for materials should be addressed to Zheng Ouyang.

Peer review information *Nature Communications* thanks the anonymous reviewers for their contribution to the peer review of this work. Peer reviewer reports are available.

Reprints and permissions information is available at <http://www.nature.com/reprints>

Publisher's note Springer Nature remains neutral with regard to jurisdictional claims in published maps and institutional affiliations.

Open Access This article is licensed under a Creative Commons Attribution 4.0 International License, which permits use, sharing, adaptation, distribution and reproduction in any medium or format, as long as you give appropriate credit to the original author(s) and the source, provide a link to the Creative Commons license, and indicate if changes were made. The images or other third party material in this article are included in the article's Creative Commons license, unless indicated otherwise in a credit line to the material. If material is not included in the article's Creative Commons license and your intended use is not permitted by statutory regulation or exceeds the permitted use, you will need to obtain permission directly from the copyright holder. To view a copy of this license, visit <http://creativecommons.org/licenses/by/4.0/>.

© The Author(s) 2023